An Impact Control Scheme Inspired by Human Reflex

Shyh-Woei Weng
Kuu-young Young*
Department of Control Engineering
National Chiao-Tung University
Hsinchu 30039, Taiwan;
e-mail: Kyoung@cc.nctu.edu.tw

Received August 31, 1995; revised June 25, 1996;
accepted July 12, 1996

In this article, we propose a control scheme to deal with unexpected impacts. Impact is inevitable when robot manipulators interact with the environment. Undesirable impacts may induce large interaction forces harmful to robot manipulators and the environment. Impacts may also excite oscillations, and even result in manipulator instability. When unexpected impacts occur, a very limited amount of time is available for control. Thus, a reflex mechanism, which emulates the functioning of human reflexes, is included in the proposed scheme. Human reflex is a kind of human action that requires no conscious effort; consequently, it responds to external stimuli without much delay. Simulations are performed to verify the effectiveness of the proposed scheme under a wide range of environmental variations and impact velocities.

この発表では、突発的な衝撃を処理する制御方法を提案する。ロボット・マニピュレータが環境と相互に作用している場合、衝撃は避けられない。望ましくない衝撃は、ロボット・マニピュレータと環境に対して悪影響を及ぼす大きな作用力を持つことがある。突発的な衝撃が起こると、制御を行う時間は非常に限られている。したがって、人間の反射動作をエミュレートした反射機構が、提案した制御方法には含められる。人間の反射は、意識的な力を必要としない人間の動作の1つであるため、外部からの刺激に対して即座に反応できる。シミュレーションを行い、提案した方法が、広い範囲の環境変化と衝撃速度において有効であることを証明する。

*To whom all correspondence should be addressed.

Journal of Robotic Systems 13(12), 837–855 (1996)

CCC 0741-2223/96/0120837-19

1. INTRODUCTION

In daily life, a person may make contact with the environment quite often. Consequently, impact is inevitable during the interaction between the limb and the environment. In general, the human motor control system handles the phenomenon of impact quite well.[1] Therefore, to let robot manipulators execute tasks that are usually performed by humans, e.g., part assembly or house cleaning, robot controllers must be able to deal with impacts. Impacts may occur in an expected or unexpected manner. For instance, Shan and Koran suggested that impacts may be expected and accommodated via their proposed motion control scheme when robot manipulators move in a cluttered but known environment.[2] On the other hand, when unexpected obstacles are present, collisions between robot manipulators and obstacles cannot be predicted in advance because no information is available prior to unexpected impacts. Consequently, a very limited amount of time is available for control during collision. In this article, we will concentrate on unexpected impacts.

Undesirable impacts may induce large interaction forces and deviate robot motions abruptly. Large impact forces may cause damage to robot manipulators and the environment, and cause robot manipulators to bounce between contact and non-contact states or even drive them into instability.[3] To alleviate the effects of unexpected impacts on robot manipulators and the environment, an impact control scheme is proposed in this article that provides stable and fast contact transition with tolerable impact force. The proposed control scheme was inspired by human reflex.[1] Reflex is a kind of human action that requires no conscious effort, and yields rapid responses to external stimuli when elicited. A reflex mechanism that emulates the functioning of human reflexes is included in the proposed scheme. The reflex mechanism basically consists of series of preprogrammed motion commands, and its implementation was inspired by the concept of human motor program. When an unexpected impact is detected during the execution of a planned motion, the reflex mechanism will be triggered and send out appropriate motion commands for impact control. After a smooth contact transition, the control will be returned to the original controller to continue the planned motion.

The rest of this article is organized as follows. In section 2, discussions about impact phenomenon and previous impact control schemes are given. In section 3, biological backgrounds of human reflexes and motor program in the human motor control system are discussed. The proposed scheme and system implementation are described in sections 4 and 5, respectively. In section 6, simulations are performed to demonstrate the effectiveness of the proposed scheme under a wide range of environmental variations and impact velocities. Finally, discussions and conclusions are given in sections 7 and 8, respectively.

2. IMPACT CONTROL

The unexpected impacts under investigation in this article are limited to situations in which robot manipulators collide with relatively immovable hard surfaces. Thus, the control aimed for is a smooth transition from free motion to constrained motion. In the former, robot manipulators move freely and do not interact with the environment. In the latter, the environment becomes part of the controlled system. Therefore, transition from free motion to constrained motion entails dynamic discontinuity characteristics. Thus, the controllers, originally designed for free motion or constrained motion, may overreact, causing the robot manipulator to bounce. In some cases, the robot manipulator might oscillate between contact and non-contact states before a stable control can be achieved. In the worst case, impact forces might even become larger and larger each time the robot manipulator contacts the environment, and eventually drive the robot manipulator into instability. In addition, impact forces outside tolerable ranges may cause damage to the robot manipulator and/or the environment. Thus, an ideal impact control scheme should be able to govern robot manipulators through impact transitions quickly and smoothly without allowing an excessively large impact force. Before we discuss development of an appropriate impact control scheme, the impact phenomenon and previous impact control schemes are reviewed below.

2.1. Impact Phenomenon

Impact occurs when two objects collide with nonzero relative velocities. From a macro point of view, impact is an impulse force adding on the colliding objects in a very short period of time. The impulse force abruptly deviates the movement of the movable

colliding object(s). From a micro point of view, the process of impact can be briefly described as follows. At first, the two objects meet, then relative motion between them continues as the areas in contact begin to deform. The interaction force between them continues increasing rapidly during this period and reaches a maximum value before the relative velocity between them drops to zero. The two objects then begin parting as the deformed surfaces begin rebounding. In the process, some energy is transferred between the colliding objects and some energy is dissipated.

When a robot manipulator collides with the environment, the stiffness of the environment and the manipulator's velocity are the two main factors contributing to impact. Figure 1 shows impact force responses under different impact velocities and different environment stiffnesses when a robot manipulator collides with an immovable surface. As expected, impact forces increase at higher impact velocities and greater environment stiffness. In addition to influencing collision magnitude, greater stiffness also shortens the impact transient time significantly, as shown in Figure 1(b). Consequently, control becomes much more difficult when the environment is rigid and the impact velocity is high. Reducing the approach velocity can reduce the effect of impact on the robot manipulator. However, it then requires a longer time to accomplish the task. On the other hand, the environment stiffness cannot be adjusted arbitrarily, and the freedom for the robot manipulator to vary its compliance is limited. These factors become more crucial under strict time constraints in impact control.

2.2. Previous Impact Control Schemes

Various impact control schemes can be divided into two main approaches: (1) preparing for impact in advance, and (2) dealing with impact during contact transience. In the first approach, Walker utilized kinematic redundancy of robot manipulators to find configurations that minimized the effects of impact at similar approach velocities.[4] Because robot configurations must be determined prior to impact, the impact point and the relationship between the robot manipulator and the environment must be known in advance. Hence, this method is suitable for tasks in environments with known structures. An and Hollerback suggested using passive compliance and damping.[5] A pliant material was added to the end-effector to provide passive damping and to help absorb impact energy. The material also lessened system stiffness effectively and made force control easier. However, system stiffness cannot be changed without physical replacement of the pliant material and the force that can be applied is limited by the material used.

In the second approach, Khatib and Burdick employed maximal active damping to help the force controller during the transition period.[6] The energy of oscillation caused by impact is dissipated by the increased damping during the transience. However, when the environment is very rigid, the energy dissi-

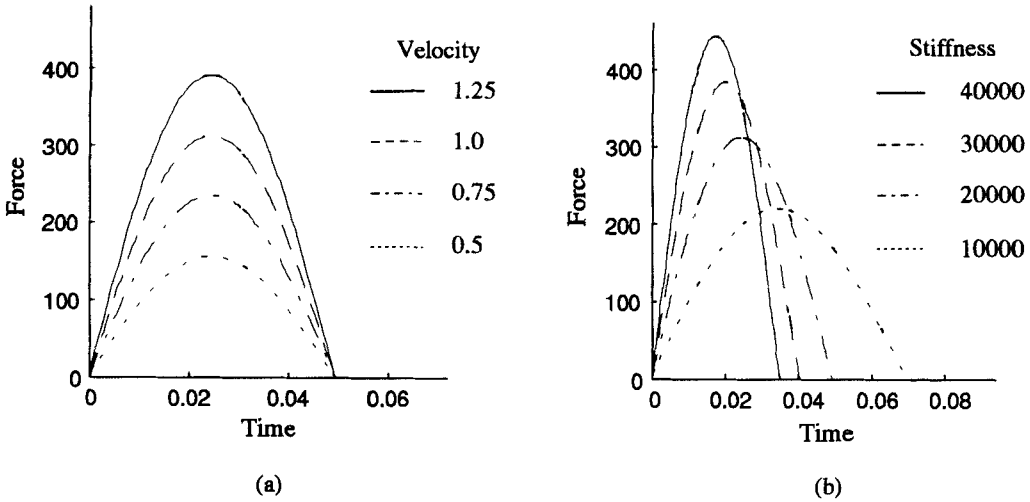

Figure 1. Impact force responses under (a) different impact velocities and (b) different environment stiffnesses.

pated by active damping during the shorter transient period is also lessened, and consequently the bounces induced by the impact may not be easy to deal with. Qian and De Schutter also introduced active linear and nonlinear damping to enable stable high gain force control in case of stiff contact.[7] Youcef-Toumi and Gutz used integral force control with velocity feedback to control impact transience.[8] The integral control acts as a low-pass filter to filter out high-frequency vibrations during transience. It can also eliminate the steady-state force following error. However, integral force control is not suitable for impacts with high-energy transfer or with an elastic environment.

Volpe and Khosla proposed dividing control into three phases: free motion, impact transience, and force control.[3] Various control strategies were adopted for each of the three phases. A negative proportional force controller with feedforward was used to govern impact transience. Mills and Lokhorst proposed a discontinuous approach for impact control.[9] A generalized dynamic system was used to design the control law and prove the stability of the proposed scheme. Hyde and Cutkosky proposed using input command preshaping to suppress oscillations during contact transition, which is basically a feedforward technique.[10] Suzuki et al. proposed a learning control scheme for impact control.[11] A learning controller was used to learn feedforward commands that helped the force feedback controller deal with impacts.

The review above indicates that most previous impact control schemes are not appropriate for dealing with unexpected impacts. They either require information about the environment, are intended for different purposes, or cannot deal with a wide range of environmental variations. On the other hand, human limbs demonstrate superior performance in impact control. Thus, emulation of human control strategies may be beneficial to robotic impact control. Human reflexes and human motor program stand especially as excellent models for robot manipulators to imitate: the former responds to external stimuli without much delay, and the latter presents a concise structure for implementing human reflex actions. Biological background material related to human reflexes and motor program in the human motor control system is discussed below.

3. HUMAN REFLEXES AND MOTOR PROGRAM

Figure 2 shows a simplified human motor control block diagram. In Figure 2, we see that human movement is governed by a hierarchical structure.[1,12] According to the goal to be achieved, the action module in the central nervous system (CNS) makes a movement plan. Appropriate motion commands are then generated by the motion command generator. The motion commands are sent to the motion command executor and the muscular system for execution. The motion command executor and the muscular system form a local control system.[13] With this hierarchical structure, the difficulty of performing complex movements can be shared by the CNS at the higher level and the local control system at the lower level.

Because feedback processing in the human motor control system is slow, long delays are experienced in the transfer of sensory information to the higher level of the hierarchy (indicated by the dashed line in Fig. 2). For slow movement, long delays may cause no serious problems when feedback control is employed by the higher level of the hierarchy; however, in dealing with fast movement, the effect

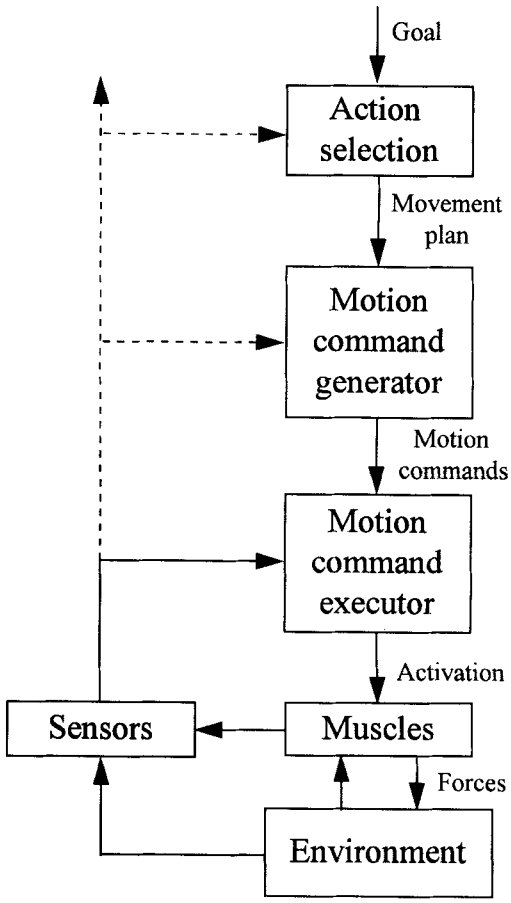

Figure 2. A simplified human motor control block diagram.

of delays cannot be ignored when the higher level of the hierarchy is governing the system in a closed-loop manner. Some biological evidence implies that fast human movement might be controlled in an open-loop manner, and a corresponding motor program concept has been proposed.[1]

In short, a motor program is an abstract representation of action that produces movement in an essentially open-loop manner. When activated, the motor program generates motion commands and sends them to the local control system, which modulates motion commands via sensory feedback, to move the limbs. To deal with a wide range of movements, the motor program should be generalized, simple to operate, and efficient in storage.[1,14] By applying the motor program concept for fast movement, the feedback path in Figure 2 can then be eliminated, because the movement is preprogrammed and controlled in an open-loop manner.

Similar to the control of fast movement, feedback control by the higher-level CNS is not appropriate for dealing with unexpected impacts. Instead, the lower-level reflex is usually invoked to tackle these impacts. Because reflex is a kind of unconscious human action in which only the lower level of the hierarchy is involved, its response to external stimuli is much faster than that of the CNS. Reflex can also be viewed as a kind of motor program prepared for some specific types of external stimuli in advance. The major difference between the motor program in the higher level of the hierarchy and that for reflex is that the former is elicited by the CNS, while the latter is triggered by unexpected external stimuli. With the distribution of intelligence between the higher-level CNS and the lower-level local control system, the human motor control system can adapt to more versatile movements and environmental variations.

4. PROPOSED SCHEME

A reflex mechanism, emulating the human reflex function, is included in the proposed scheme. The reflex mechanism is implemented using the concept of motor program. The proposed scheme is intended to provide a smooth transition when unexpected impacts occur. The ideal smooth transition adopted in the proposed scheme is defined as follows:

- No oscillations occur during transition.
- The transition period is short.
- The peak impact force is held within a prespecified range.

In the initial stage of the study, to simplify the complexity of the problem, three assumptions were made in developing the proposed scheme:

- Contact between robot manipulators and the environment is point contact.
- Environments that robot manipulators collide with are immovable hard surfaces, which can be deformed.
- No friction results from robot manipulators when robot manipulators contact the environment.

If point contact is assumed, there will be no torque present when robot manipulators contact the environment. Thus, only forces need be considered. Because no friction is present at the point of contact, the interaction force measured by the force sensor is perpendicular to the contact surface. With the immovable hard surface modeled as a stiff spring with a small damping constant, as shown in Figure 3, the relationship between the interaction force and the surface deformation can be described as

$$F_i = -B_e \Delta\dot{x} - K_e \Delta x, \tag{1}$$

where F_i is the interaction force, B_e and K_e are the damping constant and stiffness of the environment, respectively, and Δx and $\Delta\dot{x}$ stand for the amount and speed of deformation of the environment, respectively. For a hard surface, the value of K_e is quite large and that of B_e is usually very small. The direction of F_i points outward from the contact surface, because the interaction force is perpendicular to the surface.

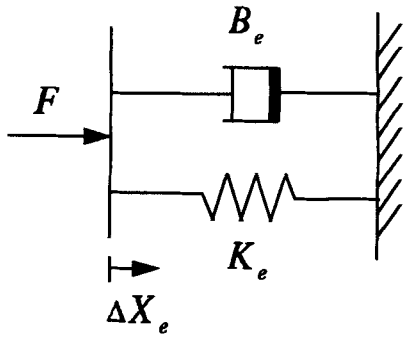

Figure 3. Environment model.

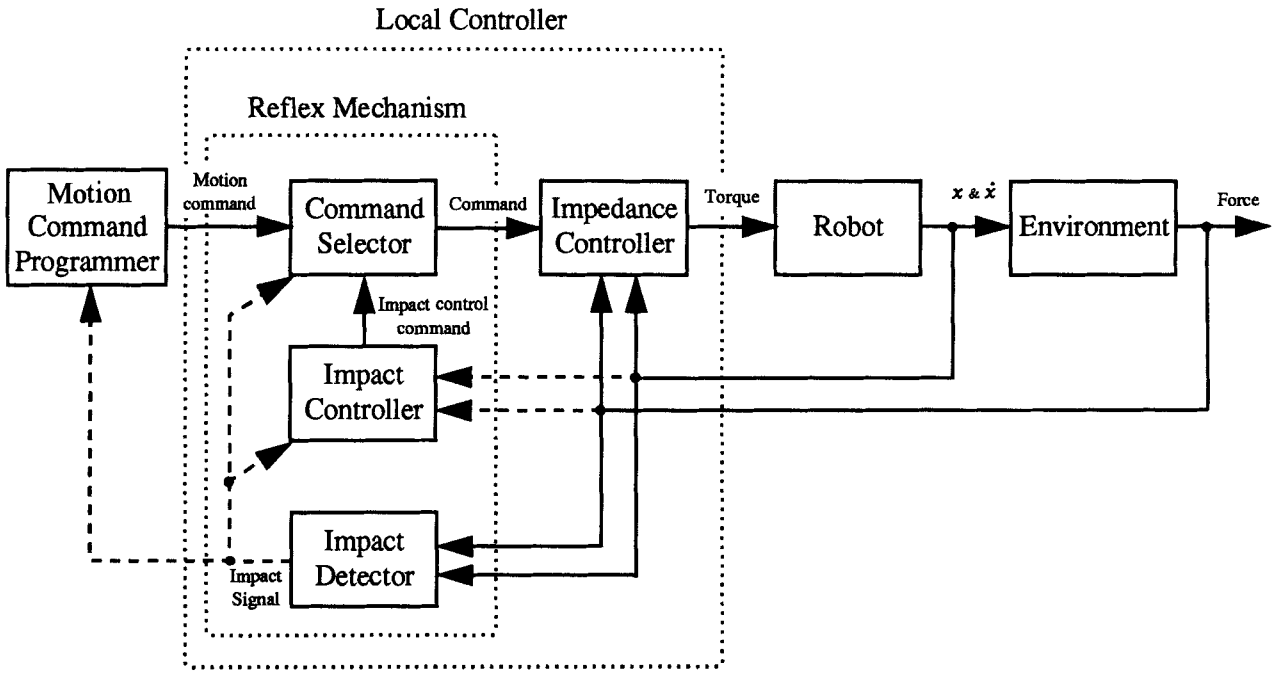

Figure 4. Functional block diagram of the proposed scheme.

4.1. System Description

Based on the ideal smooth transition and the assumptions specified above, a two-level hierarchical control scheme is proposed. Figure 4 shows the functional block diagram of the proposed scheme. A motion command programmer (MCP) serves as the higher level of the hierarchy, and a local controller, consisting of a reflex mechanism (RM) and an impedance controller, acts as the lower level. The MCP, representing the CNS, generates appropriate motion commands for planned motions. The motion commands are then executed by the impedance controller in the local controller under normal conditions.[15] When unexpected impacts occur, the RM, representing the human reflex, takes over control and generates appropriate impact control commands. Because the environment under investigation contains only immovable hard surfaces, the RM aims for a smooth transition from free motion to constrained motion. Thus, we choose an impedance controller to execute the commands from the MCP under normal conditions and the RM after unexpected impacts, because impedance control is a unified method for dealing with free and constrained motions.[15] Impedance control is also less sensitive to environmental uncertainties under unexpected impacts, when compared with other control schemes, like hybrid control.[16] After a smooth contact transition, the control is returned to the MCP from the RM. The MCP may resume the movement, or perhaps reprogram it when the effect of the impact has been serious.

As shown in Figure 4, the RM consists of three major components: an impact detector, a command selector, and an impact controller. The function of the impact detector is to detect unexpected impact by measuring contact forces. When a measured contact force is below a threshold value, the command selector allows motion commands from the MCP to pass directly to the impedance controller without involving the impact controller in the control of robot motion. When a measured contact force rises rapidly and eventually exceeds the threshold due to an unexpected impact, an impact signal is generated and sent to the command selector, the impact controller, and the MCP. The impact controller then takes over the control and generates appropriate impact control commands for the transition.

Figure 5 shows a block diagram for impact control command generation in the impact controller. In Figure 5, a number of basic impact control command patterns are installed in the impact controller in advance. These basic impact command patterns have been designed to deal with impacts that occur under certain specific conditions. To generalize these basic command patterns to accommodate a wider range of environments, the command patterns have to be scaled in both time and magnitude according to envi-

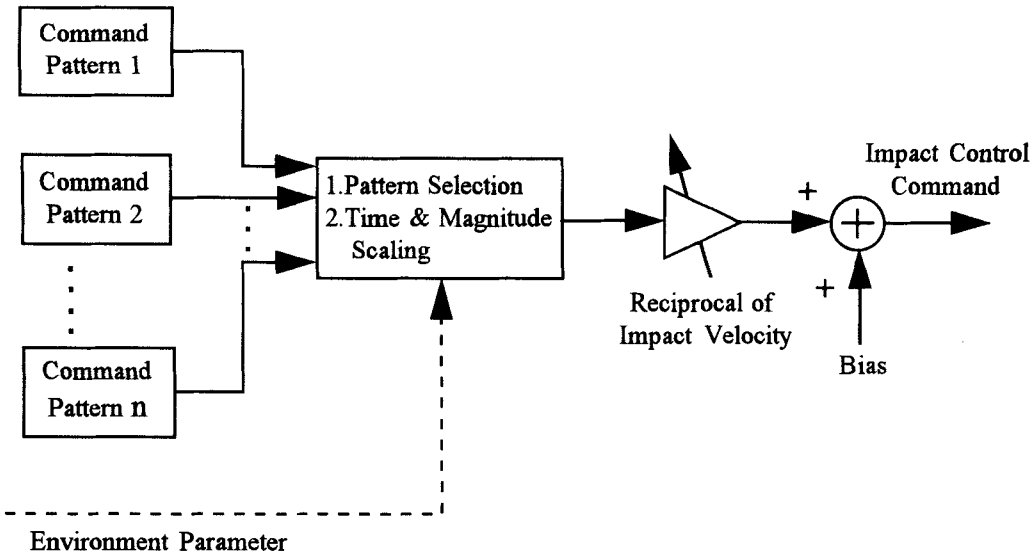

Figure 5. Block diagram for impact control command generation.

ronmental variations. In addition, the magnitudes of the command patterns are also scaled to correspond to various impact velocities.

Referring to Figure 5, when an impact occurs, the stiffness and damping of the environment are identified using the environment model described in Eq. (1). The least-square-error approach is employed for identification by using as many measurement data as are available in the short period of time allowed. Imprecision may be present in some estimates due to the limited number of measurements that can be made under such a strict time constraint. According to the identified environmental parameters, one basic impact control command pattern is selected and its corresponding time and magnitude scales determined. After the scaling above, the magnitude of the command pattern is further scaled in inverse proportion to the impact velocity. Finally, a bias term is added to the command pattern, which is set behind the contact surface a small distance from the impact point. This bias term is intended to produce a steady state force, so that the robot manipulator can maintain contact with the environment after the transition.

5. SYSTEM IMPLEMENTATION

The implementation of the proposed scheme includes three main modules: the impedance controller, the impact control command pattern derivation module, and the impact control command generalization module. The function of the impedance controller is to execute the commands from the MCP under normal conditions and the RM after unexpected impacts. Basic impact control command patterns are derived for certain specific environments and impact velocities. These basic command patterns are then generalized to deal with a wide range of environmental variations and impact velocities. Because environment estimation may not be very accurate and the number of basic impact control command patterns for generalization should be small for feasible implementation, basic command patterns should be simple, robust, and easy to generalize.

5.1. Impedance Controller

Among those robot control schemes designed to deal with the control of both position and force,[15–17] impedance control is a unified approach for both free and constrained motions. An impedance controller, instead of directly controlling the position or the force for a robot manipulator, regulates the dynamic relationship between the robot manipulator and the environment. The dynamic relationship, characterized by a target impedance, is usually formulated as a second-order system, described in Eq. (2):

$$M_d\ddot{x} + B_d\dot{x} + K_d(x - x_d) = F_e, \tag{2}$$

where M_d, B_d, and K_d are the desired matrices for inertia, damping, and stiffness, respectively, F_e is the external force vector, and x and x_d are the actual

position and the desired equilibrium-point vectors for the robot manipulator, respectively. The nonlinear control law for implementing the impedance control can be derived from the kinematic and dynamic equations for the robot manipulator along with the target impedance described in Eq. (2).[15]

To achieve effective control by using an impedance controller, the target impedance must be properly chosen. Different target impedances are used for the MCP and the RM, separately. For the MCP, the target impedance will be determined according to the given task. For the RM, it will be chosen to fulfill the ideal smooth transition defined in section 4. How the inertia, damping, and stiffness of the target impedance affect impacts are analyzed as follows. In general, high inertia tends to be not oscillatory, but may impart significant impact force. Extensive damping can suppress oscillations provoked by impact, but may lead to a longer transition time. Greater stiffness can increase the responding speed of the robot manipulator, but may increase the impact force and shorten the transient time upon impact. Basically, an overdamped target impedance is preferred to avoid oscillations during collision. An ideal target impedance for the ideal smooth transition may be determined according to the environment in contact.

5.2. Impact Control Command Pattern Derivation

As mentioned previously, basic command patterns should be simple, robust, and easy to generalize. Thus, a limited number of basic command patterns can be generalized to cover a wide range of environmental variations and impact velocities. Because there is no explicit form the ideal impact control command pattern should conform to, basic impact control command patterns will be derived via simulation and evaluation. In other words, under specific impact conditions, basic command patterns will be obtained by finding command patterns that satisfy the ideal smooth transition defined in section 4.

A fuzzy system, shown in Figure 6, is used to derive basic impact control command patterns, because the exact form of the command pattern is not very crucial and because of the capacity of the fuzzy system to formulate uncertain phenomena.[18] As described in section 2.1, impact is a dynamic process. Thus, the derived command pattern will be in the form of a continuous signal. In Figure 6, the inputs to the fuzzy system are the velocity of the end-effector and the force error between the desired steady-state force and the measured interaction force during impact; the output is the impact control command pattern. The derived impact control command pattern in Figure 6 will be sent for execution to evaluate its performance via the impact command generation process in Figure 5 and via the impact control scheme in Figure 4.

In implementing the fuzzy system, triangular membership function was chosen for the input and output fuzzy sets, described in Eq. (3):

$$\mu(x) = \begin{cases} \dfrac{R-x}{R-C} & \text{if } C \le x \le R \\ \dfrac{x-L}{C-L} & \text{if } L \le x < C \\ 0 & \text{otherwise} \end{cases} \tag{3}$$

where R, C, and L specify the right, middle, and left vertices of the triangle. The velocity and force error inputs are divided into seven and six fuzzy sets, listed in Tables I and II, respectively. Seven fuzzy sets are used for the impact control command pattern output, listed in Table III. And the rule table contains 42 inference rules, as listed in Table IV. Fuzzy rule inference is performed by the min-max operation, and the local mean of maximum (LMOM) method is used for defuzzification.[18] Thus, after the membership degree of the ith output y_i is obtained as μ_{y_i} via the fuzzy rule inference upon the two inputs, the

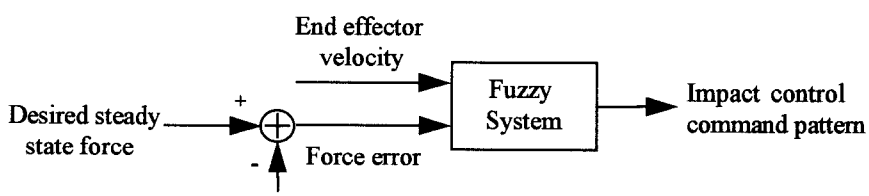

Table I. Velocity input.

	NB	NM	NS	Z	PS	PM	PB
R	−0.15	−0.05	0.00	0.05	0.15	0.30	—
C	−0.30	−0.15	−0.05	0.00	0.05	0.15	0.30
L	—	−0.30	−0.15	−0.05	0.00	0.05	0.15

Table III. Impact control command pattern output.

	NB	NM	NS	Z	PS	PM	PB
R	−0.30	−0.10	0.00	0.10	0.30	0.50	1.00
C	−0.70	−0.35	−0.15	0.00	0.10	0.30	0.70
L	−1.00	−0.50	−0.30	−0.20	0.00	0.10	0.30

value of y_i can then be computed by

$$y_i = \frac{L_{y_i} + R_{y_i}}{2} + \left(C_{y_i} - \frac{L_{y_i} + R_{y_i}}{2}\right) \mu_{y_i}, \tag{4}$$

and the output of the fuzzy system is

$$y_{out} = \frac{\Sigma\, y_i \mu_{y_i}(y_i)}{\Sigma\, \mu_{y_i}(y_i)}. \tag{5}$$

Note that those values in Tables I–IV are derived under environmental stiffness 10000 nt · m/rad. In dealing with different stiffnesses, the impact control command pattern output generated by using the fuzzy system will need to be scaled by using the gain factors listed in Table V.

The proposed scheme is implemented to deal with unexpected impacts when the environment stiffness ranges between 5000 and 80000 (nt · m/rad) and the impact velocity between 0 and 1.5 (rad/s). Two basic command patterns generated at the unit impact velocity with no environment damping will be generalized to cover the entire operating range. The first command pattern is obtained under environment stiffness 25000 nt · m/rad, and intended to cover the stiffness range of [5000, 40000] (nt · m/rad); the second pattern is under environment stiffness 60000 nt · m/rad and cover a range of [40000, 80000] (nt · m/rad). These two basic impact control command patterns are shown in Figure 7(a); their corresponding force and position responses are shown in Figures 7(b) and (c), respectively. In Figure 7(a), there are short null command periods at the beginning for both patterns to accommodate the time spent on environment identification. The magnitude of the second pattern is larger than that of the first one, because the second pattern is generated for a more rigid environment. In addition, the second pattern starts earlier and has a shorter command duration compared with the first one.

5.3. Impact Control Command Generalization

The basic impact control command patterns derived above will be generalized to accommodate a wide range of environmental variations and impact velocities via scaling of magnitudes and times. In generalization, three factors must be taken into account: the stiffness and damping of the environment and the impact velocity. However, only environment stiffness is considered in determining the scalings, because damping variation is usually small for hard surfaces. Small damping variations affect the environment identification little, because their effect on the timing of the first impact response force peak, which is crucial to environment identification, varies little. In addition, damping dissipates impact energy, thus making control easier. Hence, damping is ignored in scaling for the sake of computational and memory-utilization efficiency. Nevertheless, when damping variation is large, its effect is of concern.

Table II. Force error input.

	NVB	NB	NM	NS	Z	PS
R	−30	−10	−5	0	5	—
C	−50	−30	−15	−5	0	5
L	—	−70	−30	−10	−5	0

Table IV. Rule table.

	Velocity						
Force	NB	NM	NS	Z	PS	PM	PB
PS	Z	Z	Z	NS	NM	NB	NB
Z	Z	Z	Z	Z	NM	NB	NB
NS	Z	Z	Z	NS	NS	NM	NB
NS	Z	Z	Z	Z	NS	NM	NM
NB	Z	Z	Z	Z	Z	NS	NM
NVB	Z	Z	Z	Z	Z	NS	NS

Table V. Gain factors for different stiffnesses.

Stiffness	5000	10000	15000	20000	25000	30000	35000	40000
Factor	0.85	1.00	1.17	1.30	1.45	1.55	1.65	1.75
Stiffness	45000	50000	55000	60000	65000	70000	75000	80000
Factor	1.85	1.95	2.08	2.15	2.24	2.3	2.37	2.42

The impact velocity factor is tackled by scaling the magnitude of the command pattern in inverse proportion to the impact velocity directly, as shown in Figure 5. This is also done for computation and memory reasons; yet, performance is acceptable under this arrangement.

The fuzzy system in section 5.2 is again used to find the scalings. For the environment stiffness in the range of [5000, 80000] (nt · m/rad), starting from a stiffness value of 5000 nt · m/rad and incrementing by 5000 nt · m/rad, command patterns are derived and used as references for determining the magni-

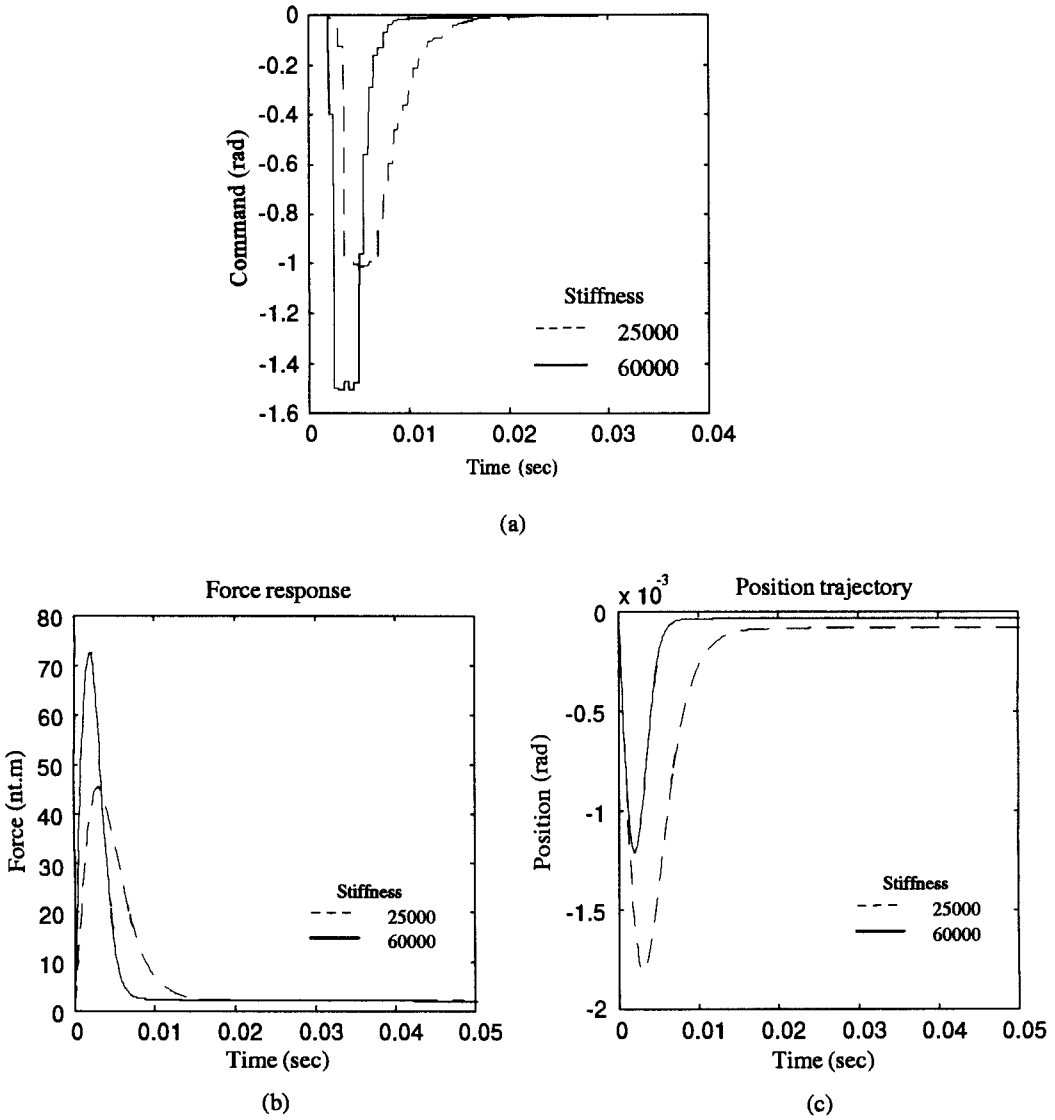

Figure 7. (a) Two basic impact control command patterns, (b) corresponding force responses, (c) corresponding position responses.

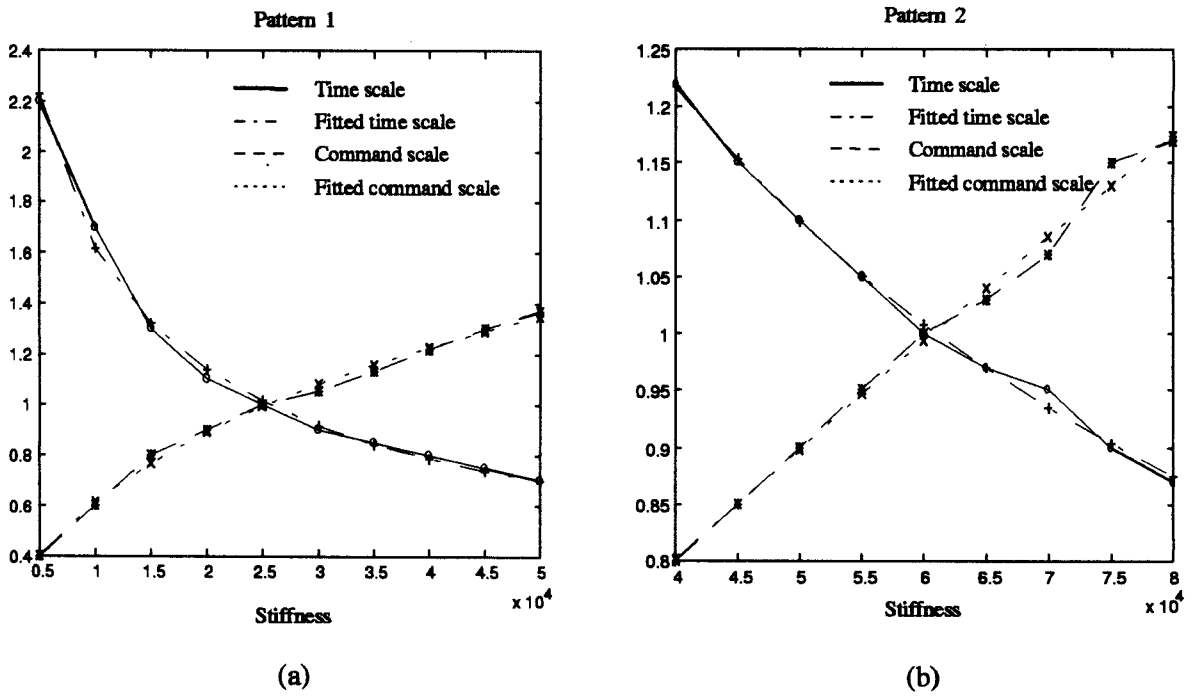

Figure 8. Time and magnitude scalings for the two basic command patterns: (a) pattern 1 and (b) pattern 2.

tude and time scalings for the two basic command patterns derived in section 5.2. It was found that command patterns generated by the fuzzy system under different sampled stiffnesses have similar shapes; thus, it is suitable to interpolate the magnitude and time scalings corresponding to the basic command patterns. A function described in Eq. (6) is then used for interpolation:

$$S(K_e) = a_2[\log(K_e)]^2 + a_1 \log(K_e) + a_0, \qquad (6)$$

where a_0, a_1, and a_2 are the coefficients of the function, and K_e is the environment stiffness. In Figure 8, the fitting curves overlaying the original discrete data are depicted, and the corresponding coefficients in the function are listed in Table VI. The least-square-error approach is used for data fitting. Obviously, other curve-fitting functions other than that in Eq. (6) can also be used.

Table VI. Coefficients for command pattern scaling.

Pattern	Scaling	a_2	a_1	a_0
Pattern 1	Time	0.0945	−2.4092	15.7058
	Magnitude	0.0521	−0.5669	1.3925
Pattern 2	Time	0.788	−2.2187	15.8800
	Magnitude	0.2232	−4.4375	21.8095

6. SIMULATION

To verify the proposed scheme, simulations based on using a single-joint robot manipulator, shown in Figure 9(a), were conducted for impact control using (i) the impedance controller alone, and (ii) the proposed scheme under various impact velocities, environment stiffnesses, and dampings. To further illustrate how the proposed scheme would be applied in cases where extra degree(s) of freedom are involved in addition to that in the impact direction, simulations were also performed using a two-joint robot manipulator, shown in Figure 9(b). All the simulations began with the robot manipulator moving in free space toward an environment an instant before collision. A 2 ms time interval was used for environment identification. The target impedance in the impact direction used in the impedance controller, as formulated using Eq. (2), was chosen to be M_d = 0.1 kg · m^2, the desired target inertia, B_d = 10 nt · m/(rad/sec), the desired damping, and K_d = 25 nt · m/rad, the desired stiffness.

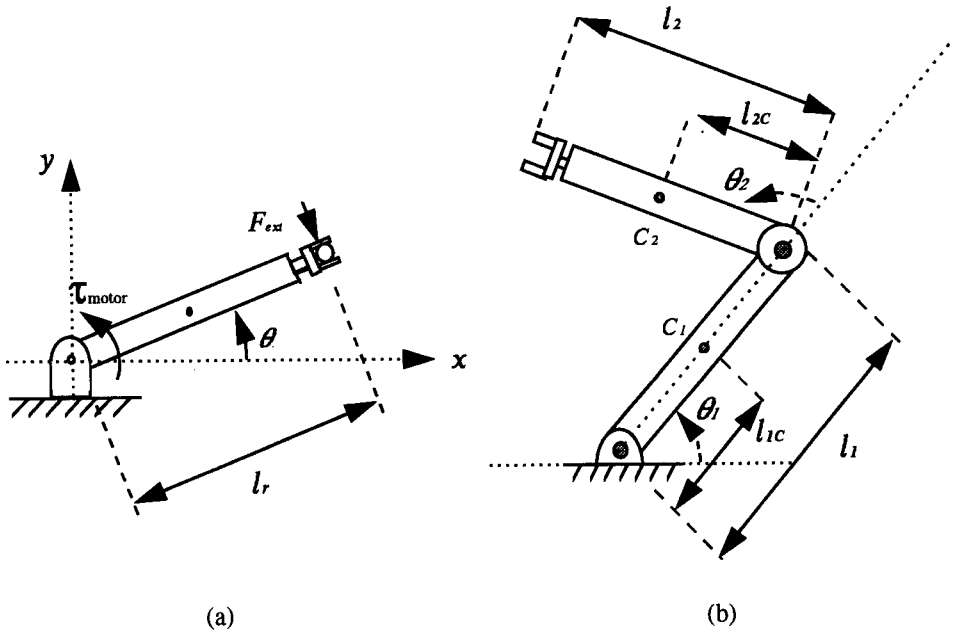

(a) (b)

Figure 9. (a) A single-joint robot manipulator, (b) a two-joint robot manipulator.

6.1. Single Joint

In the first set of simulations, the impedance controller alone was used for impact control of the single-joint robot manipulator shown in Figure 9(a). The dynamic equation for the single-joint robot manipulator is described in Eq. (7):

$$I_r\ddot{\theta} = \tau_{motor} + \tau_{ext}, \tag{7}$$

where $I_r = 0.165$ kg · m^2 is the inertia, θ is the joint angle, τ_{motor} is the torque provided by the motor, and τ_{ext} is the external force represented in the joint space. The normal vector of the environment surface points toward the positive y direction. When the joint variable θ is negative, the robot manipulator contacts the environment; when θ is positive, it is in free space.

Figure 10 shows the force and position responses under different impact velocities, environment stiffnesses, and dampings, respectively. The simulation conditions are listed in Table VII. In Figure 10(a), the robot manipulator collided with the environment with different impact velocities. The results show that the robot manipulator oscillated and long transition periods were observed even at low speeds. Figure 10(b) shows the responses when the robot manipulator collided with environments of different stiffnesses. Even when the environment was more pliable, the robot manipulator still oscillated. When the environment was more rigid, more small oscillations were observed. Figure 10(c) shows the responses when the robot manipulator collided with environments with different damping characteristics. When there was less damping, the robot manipulator oscillated frequently. Better, but not satisfactory, performance was observed when there was more damping.

Table VII. Simulation conditions using the impedance controller alone.

Condition	Env. stiffness	Env. damping	Impact velocity	θ_d
Velocity	4×10^4	5	0.1, 0.4, 0.8	−0.08
Stiffness	10^4, 4×10^4, 7×10^4	5	0.5	−0.08
Damping	4×10^4	0, 5, 10	0.5	−0.08

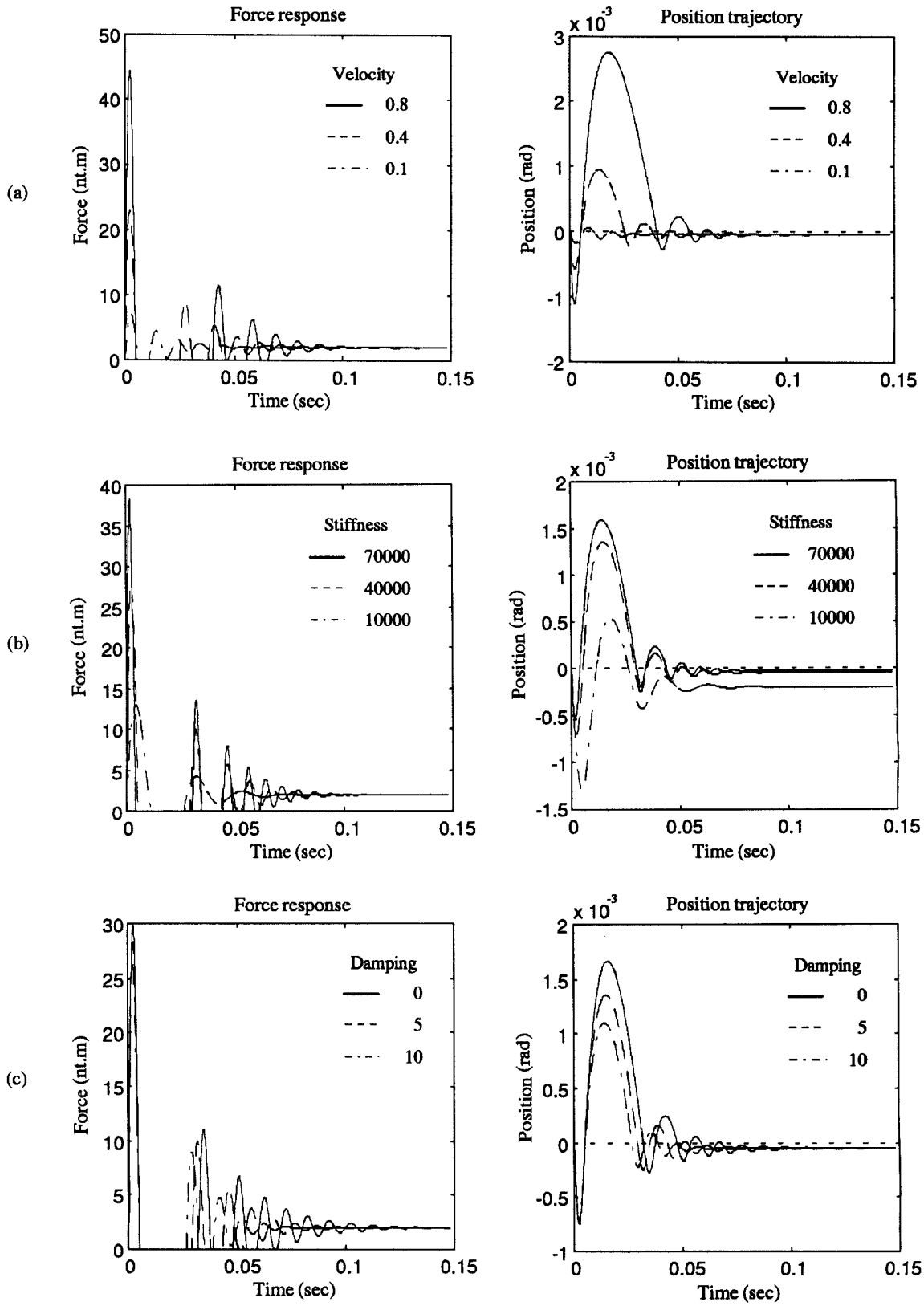

Figure 10. Impact responses using the impedance controller alone: (a) different impact velocities, (b) different environment stiffnesses, (c) different environment dampings.

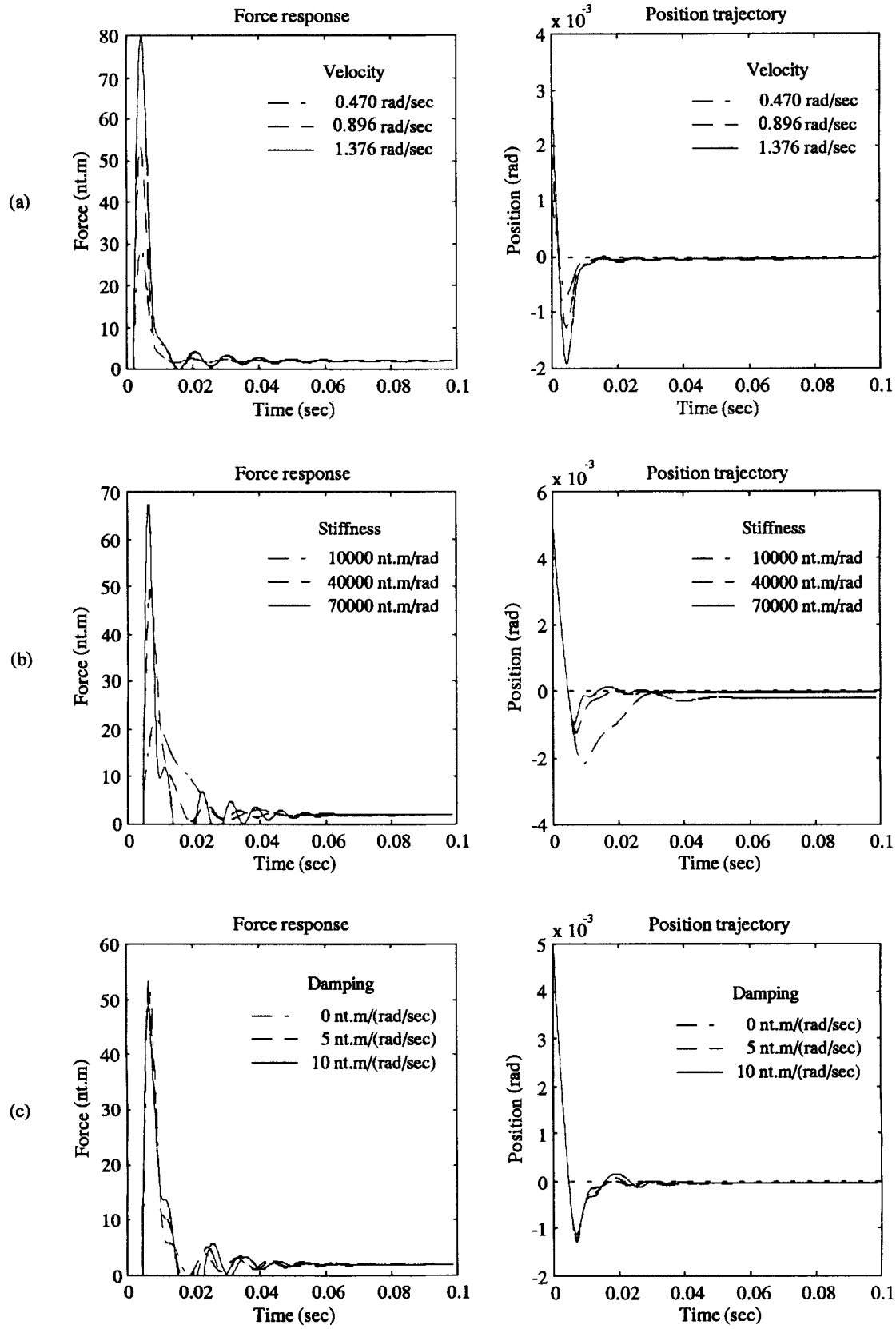

Figure 11. Impact responses using the proposed scheme (single joint): (a) different impact velocities, (b) different environment stiffnesses, (c) different environment dampings.

For comparison, a second set of simulations was performed using the proposed scheme with the same single-joint robot manipulator and the same impedance controller used above. Figure 11 shows the force and position responses under different impact velocities, environment stiffnesses, and dampings, respectively. The simulation conditions are listed in Table VIII. In Figure 11(a), the robot manipulator collided with the environment at different impact velocities. Performances yielding the ideal smooth transition defined in section 4 were obtained, even when the impact velocity was high. Figure 11(b) shows the responses when the robot collided with environments of different stiffnesses. When the environment was very rigid, the robot manipulator did bounce up with subsequent small oscillations. Yet, the performance of the proposed scheme was much better than that obtained using the impedance controller alone shown in Figure 10(b). Figure 11(c) shows the responses when the robot collided with environments with different damping characteristics. Satisfactory performances were obtained, especially for lesser degrees of damping.

Because estimation of the environment may not be very accurate due to the strict time constraints in some instances, a third set of simulations was performed to test the robustness of the proposed scheme with inaccurate environment identification. Figure 12 shows the force and position responses when the error percentage of the estimated environment stiffness was by ±25%. The simulation conditions are listed in Table IX, where it can be seen that different basic command patterns and scalings were selected according to different stiffness estimation.

Figure 12 shows performances that were not satisfactory, because the environment estimation was not accurate; yet, the performance of the proposed scheme was not worse than that obtained using the

Table VIII. Simulation conditions using the proposed scheme (single joint).

Different impact velocities				
Impact velocity	0.470	0.896	1.376	rad/s
Stiffness		42211		
Damping		0		nt · m/(rad/s)
Estimated stiffness	41960	42104	41820	nt · m/rad
Estimated damping	−2.686	−0.797	−3.418	nt · m/(rad/s)
Command pattern	Pattern 2	Pattern 2	Pattern 2	
Time scale	1.191	1.189	1.192	
Magnitude scale	0.821	0.822	0.819	
Different environment stiffnesses				
Impact velocity		0.896		rad/s
Stiffness	10^4	4×10^4	7×10^4	nt · m/rad
Damping		5		nt · m/(rad/s)
Estimated stiffness	9973	39863	69710	nt · m/rad
Estimated damping	4.810	4.245	3.682	nt · m/(rad/s)
Command pattern	Pattern 1	Pattern 1	Pattern 2	
Time scale	1.538	0.794	0.937	
Magnitude scale	0.587	1.229	1.083	
Different environment dampings				
Impact velocity		0.896		rad/s
Stiffness		42121		nt · m/rad
Damping	0	5	10	nt · m/(rad/s)
Estimated stiffness	42015	41975	41935	nt · m/rad
Estimated damping	−0.796	4.205	9.206	nt · m/(rad/s)
Command pattern	Pattern 2	Pattern 2	Pattern 2	
Time scale	1.190	1.191	1.191	
Magnitude scale	0.821	0.821	0.820	

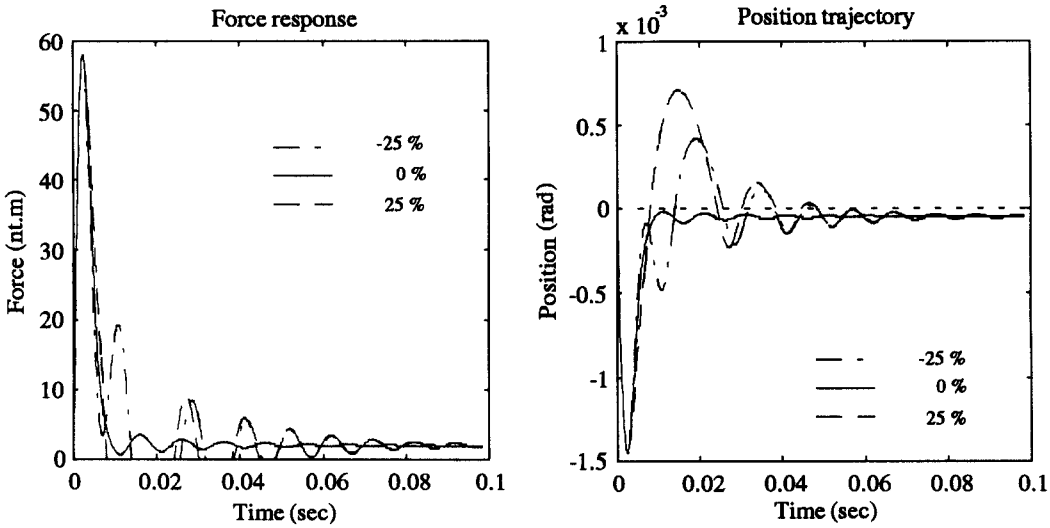

Figure 12. Impact responses using the proposed scheme when the estimated environment stiffness is not accurate.

impedance controller alone shown in Figure 10. Simulations were also performed with more inaccurate environment estimation (up to ±75%). Results similar to those shown in Figure 12 were obtained. This implies that the use of impact control commands is basically helpful in controlling impact effects, even when the timing and the magnitude of the command are not very precise due to inaccurate environment estimation. However, when the estimation deviated from the correct parameter by a wide margin, the use of the impact control command would induce larger impacts than using the impedance controller alone.

6.2. Two Joints

In the fourth set of simulations, the proposed scheme was applied to impact control using the two-joint robot manipulator shown in Figure 9(b). The dynamic equation for the two-joint robot manipulator is described in Eq. (8):

$$M(\theta)\ddot{\theta} + C(\theta, \dot{\theta}) = \tau_{motor} + J^t F_{ext}, \tag{8}$$

where

$$M(\theta) = \begin{bmatrix} M_{11} & M_{12} \\ M_{21} & M_{22} \end{bmatrix} \tag{9}$$

Table IX. Simulation conditions when the estimated environment stiffness is not accurate.

	Inaccurate identified environment stiffness			
Impact velocity		1		rad/s
Stiffness		4×10^4		nt · m/rad
Damping		0		nt · m/(rad/s)
Estimated stiffness	3×10^4	4×10^4	5×10^4	nt · m/rad
Estimated damping	0.000	0.000	0.000	nt · m/(rad/s)
Command pattern	Pattern 1	Pattern 2	Pattern 2	
Time scale	0.917	1.217	1.099	
Magnitude scale	1.080	0.802	0.898	
Error percentage of estimated stiffness	−25%	0%	25%	

$$M_{11} = m_1 l_{1c}^2 + m_2 l_1^2 + 2m_2 l_1 l_{2c} \cos\theta_2 + m_2 l_{2c}^2 + I_1 + I_2 \tag{10}$$

$$M_{12} = m_2 l_1 l_{2c} \cos\theta_2 + m_2 l_{2c}^2 + I_2 \tag{11}$$

$$M_{21} = m_2 l_{2c}^2 + m_2 l_1 l_{2c} \cos\theta_2 + I_2 \tag{12}$$

$$M_{22} = m_2 l_{2c}^2 + I_2 \tag{13}$$

$$C(\theta, \dot{\theta}) = \begin{bmatrix} -m_2 l_1 l_{2c} \sin\theta_2 \dot{\theta}_2^2 - 2m_2 l_1 l_{2c} \sin\theta_2 \dot{\theta}_1 \dot{\theta}_2 \\ m_2 l_1 l_{2c} \sin\theta_2 \dot{\theta}_1^2 \end{bmatrix} \tag{14}$$

$$\tau_{motor} = [\tau_1 \quad \tau_2]^t \tag{15}$$

$$\theta = [\theta_1 \quad \theta_2]^t, \tag{16}$$

with J standing for the Jacobian matrix; $m_1 = 4$ kg and $m_2 = 2$ kg the masses of links one and two, respectively; $I_1 = 0.09$ kg · m^2 and $I_2 = 0.02$ kg · m^2 the inertias of links one and two about their centers of mass, respectively; $l_1 = 0.5$ m, $l_2 = 0.4$ m, $l_{1c} = 0.25$ m, and $l_{2c} = 0.2$ m. When the two-joint robot manipulator contacts the environment, the normal direction is constrained by the contact surface, and the tangential direction is unconstrained. For the impedance controller, the target impedance in the normal direction is chosen as $M_d = 0.1$ kg · m^2, the desired target inertia, $B_d = 10$ nt/(m/s), the desired damping, and $K_d = 25$ nt/m, the desired stiffness; in the tangential direction, it is $M_d = 0.1$ kg · m^2, $B_d = 6$ nt/(m/s), and $K_d = 90$ nt/m. Due to the unexpected impact, the original planned equilibrium position may not be reached. A temporary equilibrium position is set as the impact position where the robot manipulator collides with the environment. The MCP at the higher level of the hierarchy in the proposed scheme shown in Figure 4, then resumes or reprograms movement from the impact position after the transition period.

The simulation conditions are listed in Table X. Figure 13 shows the simulation results. The initial configuration of the robot manipulator is as shown in Figure 13(a). In Figure 13(a), the solid lines stand for the links of the robot manipulator, the dashed line with the arrow indicates the approach direction, the dotted line specifies the contact surface, the × sign marks the original planned equilibrium point, and T and N denote the tangential and normal directions of the task coordinate system. Figure 13(b) shows the force response in the normal direction, and Figure 13(c) shows the corresponding position trajectory in the task coordinate system. In Figure 13(c), the trajectory is enlarged for illustration, and the dotted lines specify the axes of the task coordinate system. The trajectory started an instant before collision, then contacted and pressed into the environment, and finally moved back to the impact position. The performance shown in Figure 13 satisfies the ideal smooth transition defined in section 4.

Table X. Simulation conditions using the proposed scheme (two joints).

Impact velocity	(0.686, 0.297) m/s
Environment stiffness	13700 nt/m
Environment damping	0 nt/(m/s)
Estimated stiffness	13733 nt/m
Estimated damping	0.47 nt/(m/s)
Command pattern	Pattern 1
Time scale	1.334
Magnitude scale	0.717

7. DISCUSSION

In the proposed scheme, the reflex mechanism deals with the impact in an essentially open-loop manner. One major concern for open-loop control is that it is very sensitive to parameter variations. As demonstrated in the simulations above, system performance is not satisfactory when environment identification is not accurate. However, due to the strict time constraint on environment identification upon impact, accurate identification is very difficult to achieve in practical applications. Current research in human motor control suggests that the nonlinear adjustable mechanical properties of muscles may play an important role in the adaptability of human limbs to various movements, loads, and environments.[13,19] Thus, one resolution to this problem may be to use a more powerful nonlinear controller in the lower-level hierarchy rather than an impedance controller with a linear target impedance as in the proposed scheme. In other words, a more intelligent local controller capable of self-adjustment may be more appropriate for governing local behavior during impact. For instance, in ref. 20 the nonlinear PD controller for contact transient control can tune itself according to environmental variations. However, the introduction of nonlinearity may complicate system design, when a nonlinear local controller is used. Nevertheless, further study on the cooperation and intelligence distribution between the higher and lower levels of the hierarchy in an impact control system is a worthwhile future work.

A point that also deserves discussion is the application of the proposed scheme to impacts that are

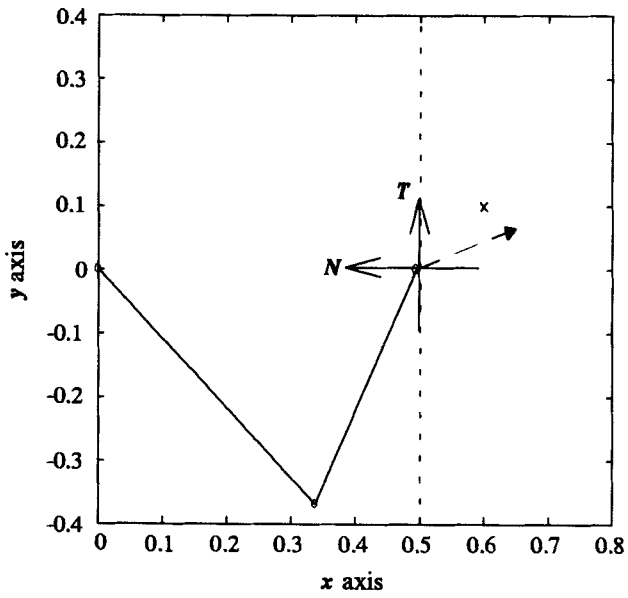

(a)

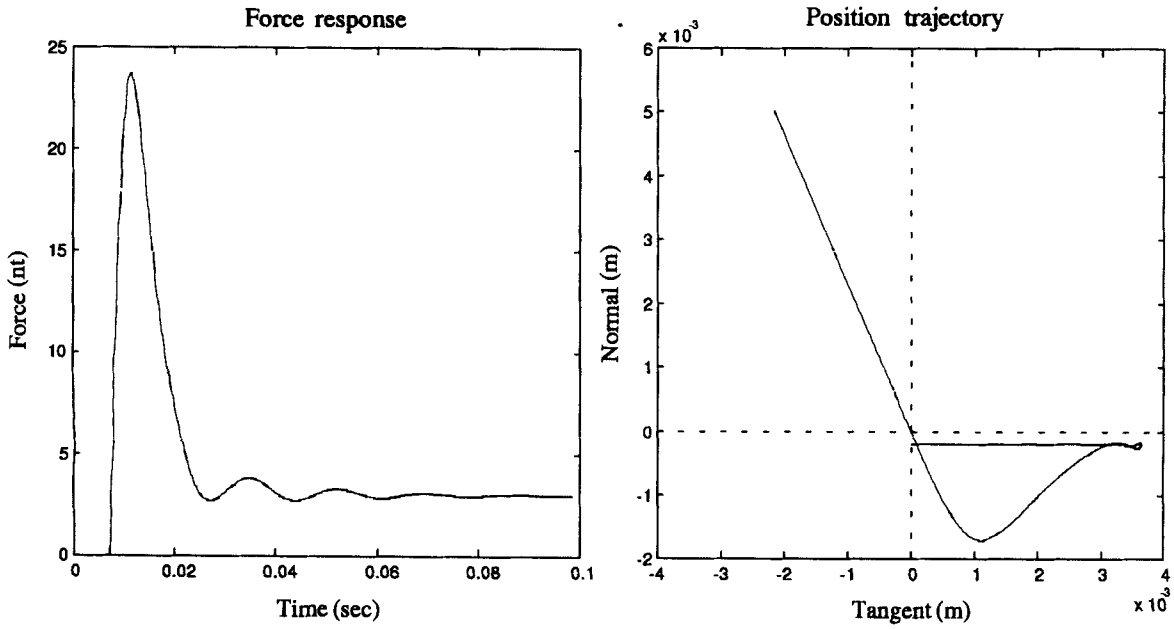

(b) (c)

Figure 13. Impact responses using the proposed scheme (two joints): (a) the configuration of the robot manipulator before collision, (b) corresponding force responses, (c) corresponding position responses.

expected. Intuitively, when a scheme can tackle an unexpected impact, it should also be capable of dealing with an expected impact. However, a controller designed for unexpected impacts may not be effective in tackling expected impacts, because only rough environment models are available via estimation for unexpected-impact control. Thus, the controller design must be conservative to accommodate a wide

range of environmental variations. On the other hand, controllers designed for expected impacts should exploit the specific properties of the known environments. Thus, the controllers will be effective for the given environments and tasks.

8. CONCLUSION

In this article, a control scheme based on a reflex mechanism, similar to human reflexes, is proposed to deal with unexpected impacts. Simulations performed demonstrate its effectiveness under a wide range of environmental variations and impact velocities. The introduction of human control strategies in the proposed scheme may be beneficial to robotic impact control. In future work, the proposed scheme will be extended to tackle more general environments under less restricted assumptions about contact.

This work was supported in part by the National Science Council, Taiwan, under Grant NSC 83-0422-E-009-065.

REFERENCES

1. R. A. Schmidt, *Motor Control and Learning: A Behavioral Emphasis*, 2nd Ed., Human Kinetics Publishers, Champaign, IL, 1988.
2. Y. Shan and Y. Koran, "Obstacle accommodation motion planning," *IEEE Trans. Rob. Autom.*, **11**(1), 36–49, 1995.
3. R. Volpe and P. Khosla, "A theoretical and experimental investigation of impact control for manipulators," *Int. J. Rob. Res.*, **12**(4), 351–365, 1993.
4. I. D. Walker, "Impact configurations and measures for kinematically redundant and multiple armed robot systems," *IEEE Trans. Rob. Autom.*, **10**(5), 670–683, 1994.
5. C. H. An and J. M. Hollerbach, "Dynamic stability issues in force control of manipulators," *Proc. IEEE Int. Conf. Rob. Autom.*, 1987, pp. 890–896.
6. O. Khatib and J. Burdick, "Motion and force control of robot manipulators," *Proc. IEEE Int. Conf. Rob. Autom.*, 1986, pp. 1381–1386.
7. H. P. Qian and J. De Schutter, "Introducing active linear and nonlinear damping to enable stable high gain force control in case of stiff contact," *Proc. IEEE Int. Conf. Rob. Autom.*, 1992, pp. 1374–1379.
8. K. Youcef-Toumi and D. A. Gutz, "Impact and force control," *Proc. IEEE Int. Conf. Rob. Autom.*, 1989, pp. 410–416.
9. J. K. Mills and D. M. Lokhorst, "Stability and control of robotic manipulators during contact/noncontact task transition," *IEEE Trans. Rob. Autom.*, **9**(3), 335–345, 1993.
10. J. M. Hyde and M. R. Cutkosky, "Controlling contact transition," *IEEE Control Syst. Mag.*, **14**(1), 25–30, 1994.
11. T. Suzuki, K. Yamada, and S. Okuma, "A fine contact motion of manipulators based on learning control," *Proc. IEEE Int. Conf. Rob. Autom.*, 1992, pp. 1461–1466.
12. M. Kawato, Y. Uno, M. Isobe, and R. Suzuki, "Hierarchical neural network model for voluntary movement with application to robotics," *IEEE Control Syst. Mag.*, **8**(2), 8–16, 1988.
13. C. C. A. M. Gielen and J. C. Houk, "A model of the motor servo: Incorporating nonlinear spindle receptor and muscle mechanical properties," *Biol. Cybern.*, **57**, 217–231, 1987.
14. K. Y. Young and S. J. Shiah, "Learning control for similar robot motions," *Proc. IEEE Int. Conf. Rob. Autom.*, 1995, pp. 2168–2174.
15. N. Hogan, "Impedance control: An approach to manipulation: Part I, II, and III," *J. Dyn. Syst. Meas. Control Trans. ASME*, **107**, 1–24, 1985.
16. M. H. Raibert and J. J. Craig, "Hybrid position/force control of manipulators," *J. Dyn. Syst. Meas. Control Trans. ASME*, **102**, 127–133, 1981.
17. S. Chiaverini and L. Sciavico, "The parallel approach to force/position control of robotic manipulators," *IEEE Trans. Rob. Autom.*, **9**(4), 361–373, 1993.
18. C. C. Lee, "Fuzzy logic in control systems: Fuzzy logic controller—Part I," *IEEE Trans. Syst. Man Cybern.*, **20**(2), 404–418, 1990.
19. C. H. Wu, K. Y. Young, K. S. Hwang, and S. Lehman, "Voluntary movements for robotic control," *IEEE Control Syst. Mag.*, **12**(1), 8–14, 1992.
20. Y. Xu, J. M. Hollerbach, and D. Ma, "A nonlinear PD controller for force and contact transient control," *IEEE Control Syst. Mag.*, **15**(1), 15–21, 1995.